MOLECULAR AND CELLULAR BIOLOGY, Sept. 2009, p. 5070–5083 Vol. 29, No. 18
0270-7306/09/$08.00+0 doi:10.1128/MCB.00138-09

The Irs1 Branch of the Insulin Signaling Cascade Plays a Dominant Role in Hepatic Nutrient Homeostasis[▽]

Shaodong Guo,[1] Kyle D. Copps,[1] Xiaocheng Dong,[1] Sunmin Park,[1] Zhiyong Cheng,[1] Alessandro Pocai,[2] Luciano Rossetti,[2] Mini Sajan,[3] Robert V. Farese,[3] and Morris F. White[1]*

Howard Hughes Medical Institute, Division of Endocrinology, Children's Hospital Boston, Harvard Medical School, Boston, Massachusetts 02115[1]; Department of Metabolic Disorders, Merck Research Laboratories, Rahway, New Jersey 07065[2]; and College of Medicine, University of South Florida, Tampa, Florida 33612[3]

Received 30 January 2009/Returned for modification 31 March 2009/Accepted 6 July 2009

We used a Cre-*loxP* approach to generate mice with varied expression of hepatic Irs1 and Irs2 to establish the contribution of each protein to hepatic nutrient homeostasis. While nutrient-sensitive transcripts were expressed nearly normally in liver lacking Irs2 (LKO2 mice), these transcripts were significantly dysregulated in liver lacking Irs1 (LKO1 mice) or Irs1 and Irs2 together (DKO mice). Similarly, a set of key gluconeogenic and lipogenic genes was regulated nearly normally by feeding in liver retaining a single *Irs1* allele without *Irs2* (DKO/1 mice) but was poorly regulated in liver retaining one *Irs2* allele without *Irs1* (DKO/2 mice). DKO/2 mice, but not DKO/1 mice, also showed impaired glucose tolerance and insulin sensitivity—though both Irs1 and Irs2 were required to suppress hepatic glucose production during hyperinsulinemic-euglycemic clamp. In contrast, either hepatic Irs1 or Irs2 mediated suppression of HGP by intracerebroventricular insulin infusion. After 12 weeks on a high-fat diet, postprandial tyrosine phosphorylation of Irs1 increased in livers of control and LKO2 mice, whereas tyrosine phosphorylation of Irs2 decreased in control and LKO1 mice. Moreover, LKO1 mice—but not LKO2 mice—that were fed a high-fat diet developed postprandial hyperglycemia. We conclude that Irs1 is the principal mediator of hepatic insulin action that maintains glucose homeostasis.

Insulin regulates systemic metabolism by activating the insulin receptor tyrosine kinase, resulting in the activation of pathways that coordinate metabolic flux, cellular growth, and survival (42, 43). Cell-based and mouse-based experiments have shown that the insulin signal is transduced largely through tyrosine phosphorylation of insulin receptor substrates 1 and 2 (Irs1 and Irs2), and other scaffold proteins including SHC, CBL, APS and SH2B, GAB1, GAB2, DOCK1, and DOCK2 (2, 4, 15, 19, 23, 27, 46). However, work with knockout mice shows that most insulin responses associated with nutrient homeostasis are mediated through Irs1 or Irs2 (42). Systemic Irs2 null mice display metabolic defects in liver, muscle, and adipose tissues (32) but develop diabetes owing to pancreatic β-cell failure (44). In contrast, systemic Irs1 null mice display growth retardation and develop peripheral insulin resistance mainly in skeletal muscle but avoid diabetes owing to robust Irs2-dependent pancreatic β-cell growth and compensatory insulin secretion (1, 38).

Insulin signaling initially promotes the storage of circulating glucose as glycogen in muscle and liver, while persistent insulin signaling promotes the conversion of excess glucose into hepatic fatty acids (35). During fasting, insulin falls while glucagon rises to stimulate hepatic glycogenolysis and gluconeogenesis to maintain circulating glucose concentrations in the normal range at the expense of hepatic fatty acid oxidation (9). Upon feeding, insulin regulates the transition from the fasting to the postprandial state by reducing the activity and concentration of rate-limiting metabolic enzymes, including phosphoenolpyruvate carboxykinase (Pck1), glucose 6-phosphatase (G6pc), and carnitine palmitoyltransferase-1 (Cpt1a) (35). This transition fails without hepatic insulin signaling, at least in part, because forkhead box O1 (Foxo1) remains active in the nucleus to prevent gene expression changes that attenuate hepatic glucose production (6). Insulin also acts upon hypothalamic neurons to suppress hepatic gluconeogenesis, but it is unknown whether this mechanism is independent of direct hepatic insulin signaling (25, 28).

Both Irs1 and Irs2 contain multiple YXXM motifs that are phosphorylated by the activated insulin receptor kinase (43). In cell-based experiments, Irs1 and Irs2 display similar capacities to bind to the 85-kDa regulatory subunits (PIK3R1 or PIK3R2) of the phosphatidylinositol 3-kinase (PI3K), which activate the associated 110-kDa catalytic subunits (PIK3C2A or PIK3C2B) that produces phosphatidylinositol-3,4,5-triphosphate (PI-3,4,5-P_3) (43). PI-3,4,5-P_3 recruits the Ser/Thr kinases PDK1 and Akt to the plasma membrane where Akt is activated by PDK1-mediated phosphorylation (22). Cell lines derived from embryonic hepatocytes suggest that Irs2 is the principal mediator of the PI3K→Akt cascade in the liver (33, 41). Regardless, recent work in adult mouse liver or isolated hepatocytes shows that Akt is activated by Irs1 and Irs2, in either case promoting the phosphorylation of glycogen synthase kinase-3β (GSK3β) and GSK3α, FOXO transcription factors, and components of the mTOR pathway (5, 6, 16). Activation of atypical protein kinase C isoforms by insulin-stimulated PI3K→PDK1 signaling contributes to hepatic fatty acid homeostasis and, unexpectedly, depends entirely upon the Irs2 branch of the insulin signaling cascade (7, 37).

* Corresponding author. Mailing address: Howard Hughes Medical Institute, Division of Endocrinology, Children's Hospital Boston, Harvard Medical School, Karp Family Research Laboratories, Rm. 4210, 300 Longwood Avenue, Boston, MA 02115. Phone: (617) 919-2846. Fax: (617) 730-0244. E-mail: morris.white@childrens.harvard.edu.

▽ Published ahead of print on 13 July 2009.

Recent data suggest that Irs2 functions mainly during fasting and immediately after feeding to suppress hepatic glucose output (16), whereas Irs1 functions mainly during feeding to regulate hepatic glucose homeostasis and promote lipogenesis (16). Indeed, acute reduction of *Irs2* expression—accomplished via adenovirus-mediated short hairpin RNA (shRNA) delivery—causes mild steatosis (40). Thus, persistent Irs1 signaling without Irs2 might promote excess lipid synthesis. We used the Cre-*loxP* approach to produce mice with different hepatic concentrations of Irs1 or Irs2. This experimental approach can reveal how mice adapt to partial Irs1 or Irs2 deficiency—which, unlike the acute reduction achieved by transient expression of shRNA (40), might resemble the physiologic state developed during the prolonged period of metabolic dysregulation preceding overt type 2 diabetes.

MATERIALS AND METHODS

Animals. Generation of animals with floxed (flanked by *loxP*) *Irs2* has been described previously (17); a similar strategy was used to generate the floxed *Irs1* allele (6). Mice of six different genotypes were selected and analyzed in this study. Mice homozygous for the floxed *Irs1* and *Irs2* alleles ($Irs1^{lox/lox}$::$Irs2^{lox/lox}$) were used as control (CNTR) mice. LKO1 mice are liver-specific *Irs1* knockout mice, while LKO2 mice are liver-specific *Irs2* knockout mice; each was generated by breeding the respective floxed mice ($Irs1^{lox/lox}$ or $Irs2^{lox/lox}$) with *Alb-Cre* transgenic mice [Jackson Laboratory strain B6.Cg-Tg(Alb-cre)21 Mgn/J] that express the *Cre* recombinase cDNA from the rat albumin promoter (31). The DKO mice are those in which both *Irs1* and *Irs2* are simultaneously deleted in the liver ($Irs1^{lox/lox}$::$Irs2^{lox/lox}$::*Alb-Cre*). DKO/1 mice are DKO mice in which one wild-type (+) allele of *Irs1* is retained ($Irs1^{+/lox}$::$Irs2^{lox/lox}$::*Alb-Cre*), while DKO/2 mice are DKO mice in which one wild-type *Irs2* allele is retained ($Irs1^{lox/lox}$::$Irs2^{+/lox}$::*Alb-Cre*). All the mice were maintained on a mixed background derived from C57BL/6J and 129/Sv. Genotyping was performed by PCR using genomic DNA isolated from the tail tip as previously described in references 6 and 17. Animals were housed on a 12-h/12-h light/dark cycle and were fed a standard rodent chow ad libitum. For high-fat diet (HFD) feeding, 4-week-old male mice were fed a diet containing 45% fat-derived calories (D12451; Research Diet) for 12 weeks. All protocols for animal use and euthanasia were approved by the Institutional Animal Care and Use Committee of Children's Hospital Boston and in accordance with NIH guidelines.

Metabolic analysis. Blood glucose levels were measured in random-fed (ad libitum) or overnight-fasted mice using a glucometer (Elite XL; Bayer). Plasma insulin and leptin levels were measured using rat insulin and leptin enzyme-linked immunosorbent assay (Crystal Chem Inc.), respectively. Plasma triglycerides, free fatty acids, and total cholesterol from overnight-fasted mice were measured using the L-type triglyceride, nonesterified fatty acid, and cholesterol E kits from Wako Diagnostics (Richmond, VA), respectively. Serum albumin levels were assessed using BCG reagent (Bioassay System, Hayward, CA). Glucose tolerance tests were performed on overnight-fasted mice. Animals were injected intraperitoneally (i.p.) with D-glucose (2 g/kg of body weight), and blood glucose levels were measured at indicated time points. For insulin tolerance tests, mice were fed ad libitum, and diluted insulin (1 U/kg Humulin R; Lilly) was injected i.p.; blood glucose concentrations were measured at 0, 15, 30, and 60 min after insulin injection. Bone mineral density and fat accumulation were determined using dual-energy X-ray absorptiometry with a Lunar Piximus II mouse densitometer (GE LUNAR Corp., Madison, WI) as described by the manufacturer. Mice were anesthetized using Avertin (0.25 mg/g body weight, i.p.) before scanning. Hepatic glycogen content in liver was analyzed in fed mice, and hepatic triglyceride concentrations were analyzed in overnight-fasted mice, as previously described (6).

Hyperinsulinemic-euglycemic clamp. To assess glucose metabolism in vivo, mice were subjected to hyperinsulinemic-euglycemic clamp analysis after catheters were implanted into the right jugular vein 5 days prior to the clamp. The procedure was performed essentially as previously described for overnight-fasted mice (17).

Intracerebroventricular (ICV) insulin stimulation with pancreatic insulin clamp. For ICV insulin infusion and pancreatic insulin clamp, a catheter was implanted in the third cerebral ventricle 3 weeks prior to the clamp experiment. Additional catheters were implanted in the right jugular vein and left carotid artery a week before the clamp. The clamp procedure was performed as previously described (30).

Antibodies. Antibodies against Akt, Foxo1, Gsk3β/α, ribosomal S6 kinase (S6K), and β-actin or phosphospecific antibodies against Akt(T308), Akt(S473), Foxo1(S256), Gsk3β(S9), and S6K(T389) were obtained from Cell Signaling Technology. Antibodies against Irs1, Irs2, and p85 were obtained from Millipore (Billerica, MA).

RNA isolation and quantitative real-time PCR. Total RNA was isolated from liver using the Trizol reagent (Invitrogen) according to the manufacturer's protocol. For real-time PCR analysis, 1 μg of total RNA was treated with RNase-free DNase and subsequently reverse transcribed with random hexamer primers (Bio-Rad). Relative mRNA abundance levels normalized to cyclophillin levels were determined with the threshold cycle ($\Delta\Delta C_T$) method after amplification, using an iCycler IQ real-time PCR detection system (Bio-Rad) and SYBR green (Bio-Rad). The data are presented as means ± standard errors of the means (SEM).

Affymetrix GeneChip analysis. Liver mRNA expression in LKO1, LKO2, and DKO mice fasted for 16 h ($n = 2$) or fed for 4 h ($n = 2$) was determined on MG430 2.0 GeneChips (Affymetrix); for CNTR mice, a total of six fasted and six fed mice were used. RNA labeling and microarray hybridizations were performed at the Harvard Medial School Biopolymers Facility, using the Affymetrix model 450 fluidics station and model 3000 scanner. Affymetrix Mircroarray Suite 5.0 was used to generate cell intensity (CEL) files that were analyzed by robust multichip average analysis implemented in GeneSpring 7.2 (Agilent Technologies).

Immunoprecipitation and Western blot analysis. Livers were removed and homogenized in homogenization buffer (25 mM Tris-Cl [pH 7.4], 50 mM sodium pyrophosphate, 100 mM sodium fluoride, 10 mM EDTA, 1% NP-40, 1 mM phenylmethylsulfonyl fluoride, 10 mM sodium orthovanadate, 10 μg/ml aprotinin, and 10 μg/ml leupeptin). Samples were allowed to solubilize for 30 min on ice, and particulate matter was removed by centrifugation at 14,000 × *g* for 15 min at 4°C. Immunoprecipitations and Western blot analyses of insulin signaling proteins were performed as previously described (11) using 100 μg (immunoblots) or 500 μg (immunoprecipitations) of each liver lysate. Liver lysates or immunoprecipitates were resolved by sodium dodecyl sulfate-polyacrylamide gel electrophoresis and transferred to nitrocellulose membranes for immunoblotting with specific antibodies. Representative blots, developed using enhanced chemiluminescence, were quantitated using ImageQuant TL (2003) software.

aPKC activity. Atypical protein kinase C (aPKC) activity was measured as previously described (37).

Statistics. All data are presented as means ± SEM or as estimated marginal means ± SEM determined by generalized linear regression (SPSS, version 16.0). Pairwise comparisons of the estimated marginal means were made, and $P < 0.05$ was taken as a significant difference. The Bonferroni method was used to adjust the observed significance levels for the fact that multiple contrasts were being tested. Serial measurements made during glucose and insulin tolerance tests were summarized by determining the area under the curve using Medcalc v10.0 (6).

RESULTS

Differential regulation of gene expression by hepatic Irs1 and Irs2. To distinguish the contributions of Irs1 and Irs2 in the liver, we investigated the effect of 4 h of feeding upon the concentration of Irs1/2-sensitive transcripts in livers of mice lacking hepatic Irs1 (LKO1) or Irs2 (LKO2). To select a set of informative transcripts that depended upon Irs1 or Irs2 signaling for normal expression, we analyzed previously published results obtained from these mice, using Affymetrix MOE430 GeneChips (ArrayExpress database accession number E-MEXP-1649) (6). Thousands of probe sets were previously reported to change significantly across all possible test conditions. In this analysis, we restricted the list to the 319 probe sets (109 genes) that changed significantly—more than ±1.5-fold (false discovery rate [FDR] of <0.01)—in CNTR liver but changed less than ±1.4-fold—in practice not at all (FDR > 0.05)—between fasted and fed DKO mouse liver (Fig. 1). This set of transcripts contained well-known insulin-sensitive genes, including the


log2[fed/fast]
log2[fast]
Name
ID
CNTR LKO1 LKO2 DKO
CNTR LKO1 LKO2
Description
Correlation Coefficient (r) 1 0.86 0.95 0.68 1 0.63 0.78
95% CI 0.79-0.90 0.92-0.97 0.55-0.78 0.50-0.73 0.69-0.84
IGFBP1 1418918_at insulin-like growth factor binding protein 1
ZBTB16 1459557_at zinc finger and BTB domain containing 16
SLC7A2 1436555_at solute carrier family 7 (y+ system), member 2
C16ORF5 1460172_at chromosome 16 open reading frame 5
IL6R 1452416_at interleukin 6 receptor
ADK 1456960_at adenosine kinase
AGTR1 1436739_at angiotensin II receptor, type 1
GFRA1 1439015_at GDNF family receptor alpha 1
TAT 1451557_at tyrosine aminotransferase
TAOK3 1435964_a_at TAO kinase 3
TOX 1458974_at thymocyte selection-associated high mobility group box
G6PC 1417880_at glucose-6-phosphatase, catalytic subunit
SCARB1 1416050_a_at scavenger receptor class B, member 1
ABCC3 1443206_at ATP-binding cassette, sub-family C (CFTR/MRP), member 3
ABCB4 1449818_at ATP-binding cassette, sub-family B (MDR/TAP), member 4
NUDT4 1418505_at nudix (nucleoside diphosphate linked moiety X)-type motif 4
GCH1 1420499_at GTP cyclohydrolase 1 (dopa-responsive dystonia)
RBMS1 1418703_at RNA binding motif, single stranded interacting protein 1
PPARGC1A 1460336_at peroxisome proliferator-activated receptor γ, coactivator 1α
GRN 1448148_at granulin
FLNB 1445534_at filamin B, beta (actin binding protein 278)
CTSL2 1451310_a_at cathepsin L2
CEBPB 1418901_at CCAAT/enhancer binding protein (C/EBP), β
RBPMS 1459078_at RNA binding protein with multiple splicing
ATXN2 1460653_at ataxin 2
ELK4 1427162_a_at ELK4, ETS-domain protein (SRF accessory protein 1)
FARP2 1435985_at FERM, RhoGEF and pleckstrin domain protein 2
PCK1 1423439_at phosphoenolpyruvate carboxykinase 1 (soluble)
TNFRSF1B 1418099_at tumor necrosis factor receptor superfamily, member 1B
SGK2 1418739_at serum/glucocorticoid regulated kinase 2
INSR 1434446_at insulin receptor
HMGA1 1416184_s_at high mobility group AT-hook 1
NR1I2 1425723_at nuclear receptor subfamily 1, group I, member 2
GNE 1448810_at GlcNAc (UDP-N-acetyl)-2-epimerase/N-acetylmannosamine kinase
PECI 1431012_a_at peroxisomal D3,D2-enoyl-CoA isomerase
GNS 1446861_at glucosamine (N-acetyl)-6-sulfatase (Sanfilippo disease IIID)
GALNT2 1452182_at UDP-N-Ac-α-D-GalNAc:polypeptide N-Ac-galactosaminyltransferase 2
MVK 1418052_at mevalonate kinase
SYT1 1433884_at synaptotagmin I
UBE2B 1439477_at ubiquitin-conjugating enzyme E2B (RAD6 homolog)
PPM1A 1415678_at protein phosphatase 1A, magnesium-dependent, alpha isoform
AFF4 1450031_at AF4/FMR2 family, member 4
ARHGAP5 1423194_at Rho GTPase activating protein 5
KLF9 1436952_at Kruppel-like factor 9
SIRT3 1417892_a_at sirtuin-3
PPARGC1B 1449945_at peroxisome proliferator-activated receptor gamma, coactivator 1 beta
NFE2 1452001_at nuclear factor (erythroid-derived 2), 45kDa
PPP3CA 1452056_s_at protein phosphatase 3 (formerly 2B), catalytic subunit, alpha isoform
CPT1A 1438156_x_at carnitine palmitoyltransferase 1A (liver)
GK 1422703_at glycerol kinase
AIM1 1426942_at absent in melanoma 1
RND1 1455197_at Rho family GTPase 1
RBL2 1418146_a_at retinoblastoma-like 2 (p130)
CASP6 1415995_at caspase 6, apoptosis-related cysteine peptidase
NFIA 1440660_at nuclear factor I/A
ACACA 1434185_at acetyl-Coenzyme A carboxylase alpha
PDE7B 1445539_at phosphodiesterase 7B
MXI1 1450376_at MAX interactor 1
ABCG8 1420656_at ATP-binding cassette, sub-family G, member 8 (sterolin 2)
NIPBL 1437158_at Nipped-B homolog
PCBP4 1433658_x_at poly(rC) binding protein 4
VEGFC 1440739_at vascular endothelial growth factor C
CCNI 1448334_a_at cyclin I
SIP1 1451044_at survival of motor neuron protein interacting protein 1
WASL 1439832_at Wiskott-Aldrich syndrome-like
TM4SF4 1424962_at transmembrane 4 L six family member 4
FUS 1455831_at fusion (involved in t(12;16) in malignant liposarcoma)
NSDHL 1416222_at NAD(P) dependent steroid dehydrogenase-like
PPP1R3B 1436590_at protein phosphatase 1, regulatory (inhibitor) subunit 3B
PROK1 1443505_at prokineticin 1
ACAT2 1435630_s_at acetyl-Coenzyme A acetyltransferase 2
ABCG5 1419393_at ATP-binding cassette, sub-family G, member 5 (sterolin 1)
LPP 1438271_at LIM domain containing preferred translocation partner in lipoma
SC5DL 1424709_at sterol-C5-desaturase-like
CDC34 1434879_at cell division cycle 34 homolog (S. cerevisiae)
ACTB M12481_3_at actin, beta
DHCR24 1451895_a_at 24-dehydrocholesterol reductase
DHCR7 1448619_at 7-dehydrocholesterol reductase
CTPS 1416563_at CTP synthase
HPGD 1419906_at hydroxyprostaglandin dehydrogenase 15-(NAD)
IFI35 1445897_s_at interferon-induced protein 35
PRPF31 1457083_at PRP31 pre-mRNA processing factor 31 homolog
PCSK9 1437453_s_at proprotein convertase subtilisin/kexin type 9
MVD 1417303_at mevalonate (diphospho) decarboxylase
PER2 1445892_at period homolog 2
BYSL 1450742_at bystin-like
GCS1 1422489_at glucosidase I
ONECUT1 1456974_at one cut homeobox 1
RBM39 1438420_at RNA binding motif protein 39
RCAN1 1416600_a_at regulator of calcineurin 1
FDFT1 1448130_at farnesyl-diphosphate farnesyltransferase 1
BCL3 1418133_at B-cell CLL/lymphoma 3
XBP1 1420012_at X-box binding protein 1
TUBB 1416256_a_at tubulin, β
PITPNC1 1455204_at phosphatidylinositol transfer protein, cytoplasmic 1
DNAJA1 1416288_at DnaJ (Hsp40) homolog, subfamily A, member 1
DNAJB2 1448657_a_at DnaJ (Hsp40) homolog, subfamily B, member 2
LSS 1420013_s_at lanosterol synthase
DKC1 1438016_at dyskeratosis congenita 1, dyskerin
CACYBP 1452047_at calcyclin binding protein
HMGCR 1427229_at 3-hydroxy-3-methylglutaryl-Coenzyme A reductase
TUBB2C 1423642_at tubulin, beta 2C
CYP51A1 1450646_at cytochrome P450, family 51, subfamily A, polypeptide 1
HSP90AA1 1438902_a_at heat shock protein 90kDa alpha (cytosolic), class A member 1
HSPH1 1425993_a_at heat shock 105kDa/110kDa protein 1
GCK 1425303_at glucokinase
FDPS 1423418_at farnesyl diphosphate synthase
SQLE 1415993_at squalene epoxidase
SC4MOL 1423078_a_at sterol-C4-methyl oxidase-like
NUDT7 1431302_a_at nudix (nucleoside diphosphate linked moiety X)-type motif 7
log2 [fast]
-0.22 0.29 CNTR
-0.64 0.33 LKO1
-0.69 0.38 LKO2
log2 [fed-fast]
-3.92 2.76 CNTR
-4.08 2.54 LKO1
-5.33 3.64 LKO2
-0.48 0.47 DKO

Igfbp1, G6pc, Pck1, Pgc1α, Xbp1, and Gck genes (Fig. 1). Inspection of the heat map showed that the responses of these transcripts to feeding were similar in CNTR and LKO2 mice, as Pearson's correlation coefficient (r) was nearly perfect ($r = 0.95$; 95% confidence interval [CI], 0.92 to 0.97; $P < 0.0001$). In comparison, the response of the reporter transcripts to feeding in LKO1 mice was less correlated to that in the CNTR ($r = 0.86$; 95% CI, 0.79 to 0.90; $P < 0.001$). Thus, either Irs1 or Irs2 could regulate the transition of hepatic gene expression from the fasted to postprandial state, but Irs1 was required for a near normal response.

Since Irs2 was proposed recently to play a dominant role during fasting (16), we compared the concentrations of the reporter transcripts specifically in fasted liver samples (Fig. 1). Inspection of the heat map indicated that deletion of either Irs1 or Irs2 influenced the overall expression of these reporter transcripts during fasting. Since the Pearson's correlation coefficients were indistinguishable between LKO1 and LKO2 mice, we conclude that both Irs1 and Irs2 contribute to the regulation of these genes during fasting (Fig. 1).

Feeding-stimulated signaling in DKO/1 and DKO/2 mice. Previous work shows that liver-specific knockout of Irs1 or Irs2 has a moderate effect upon hepatic insulin action at the physiologic level (5, 6, 16). To establish whether incomplete loss of Irs1 or Irs2 affects the hepatic insulin response, we used a Cre-*loxP* strategy to produce mice that retained one allele of Irs1 without Irs2 (DKO/1 mice) or one allele of Irs2 without Irs1 (DKO/2 mice). Immunoblotting confirmed the complete absence of Irs1 and Irs2 in the DKO liver (Fig. 2A and B). Compared to liver extracts from CNTR mice, DKO/1 liver extracts had a low concentration of Irs1 and undetectable Irs2, whereas DKO/2 liver extracts had a low concentration of Irs2 without Irs1 (Fig. 2A and B). The phosphorylation of several proteins in the Irs1/2→PI3K→Akt signaling cascade was analyzed in liver extracts from mice fasted 20 h or mice fasted 20 h and allowed access to food for a further 4 h (Fig. 2C to G). In CNTR mice, feeding increased the phosphorylation of Akt (T308 and S473), Foxo1(S253), GSK3β(S9), and S6K(T389). As previously shown, the phosphorylation of Akt(T308) and Foxo1(S253) was completely absent in the fed DKO liver (Fig. 2C and E). In contrast, Akt(S473) phosphorylation was elevated significantly in fasted DKO liver but did not increase during the postprandial period (Fig. 2D). Feeding significantly stimulated phosphorylation of Akt(T308) in DKO/1 or DKO/2 liver; however, in the fasted state, Akt(T308) phosphorylation was significantly higher in the DKO/1 liver (Fig. 2C). Regardless, downstream phosphorylation of Foxo1(S253) was indistinguishable in DKO/1 and DKO/2 livers under fasting or postprandial conditions (Fig. 2E). Finally, stimulation of GSK3β(S9) and S6K(T389) phosphorylation by feeding was detected in DKO/1, DKO/2, and DKO liver (Fig. 2F and G).

Hepatic gene expression in DKO/1 and DKO/2 mice. We investigated the concentrations of transcripts encoding specific insulin-sensitive genes—including the G6pc, Pck, Gck, Fasn, Hmgcr, Acc, Srebp1c, and Srebp2 genes in livers from CNTR mice or from DKO/1, DKO/2, and DKO mice. Under fasting conditions, the expression of the tested genes in DKO/1 and DKO/2 livers was barely different than that in the CNTR (Fig. 3A to H). As expected, the concentration of G6pc and Pck transcripts decreased significantly in CNTR mice after feeding—consistent with the suppression of gluconeogenesis by insulin (Fig. 3). In contrast, the transcript concentrations of Gck, Fasn, Acc, Hmgcr, Srebp1c, and Srebp2 increased after feeding CNTR mice, which is consistent with the utilization of glucose by the postprandial liver for the synthesis of glycogen, fatty acids, and cholesterol (Fig. 3). In comparison, the effect of feeding upon these genes was largely lost in DKO liver, confirming that the postprandial concentrations of these transcripts were regulated largely by Irs1 or Irs2 signaling (Fig. 3). In several cases—G6pc, Pck, Gck, Fasn, and Srebp1c (Fig. 3A, C, E, G, and F)—the retention of Irs1 (DKO/1 mice) allowed a more normal postprandial response than did the retention of Irs2 (DKO/2 mice). In the case of Hmgcr and Srebp2, the response to feeding was significantly reduced in both DKO/1 and DKO/2 livers. Thus, both Irs1 and Irs2 contributed to gene expression in the liver, but in most cases, Irs1 appeared to be dominant, as suggested by the Affymetrix analysis results (Fig. 1).

Metabolic regulation in DKO/1 and DKO/2 mice. As previously shown, DKO mice were about 30% smaller than CNTR mice (Fig. 4A). Although DKO/1 and DKO/2 mice were slightly smaller than the CNTR mice, the difference did not reach statistical significance (Fig. 4A). At 6 weeks of age, the DKO mice displayed ~40% greater adiposity and ~20% less bone mineral density than CNTR mice, whereas adiposity and bone density were indistinguishable between CNTR, DKO/1, and DKO/2 mice (Fig. 4B and C). In 8-week-old DKO mice, fasting plasma concentrations of insulin and leptin and fasting blood glucose concentrations were significantly elevated (Fig. 4D to F), whereas the concentrations of triglyceride, free fatty acids, and free cholesterol decreased (Fig. 4G to I). In contrast, each of these measures was normal in the DKO/2 and DKO/1 mice (Fig. 4D to I), as well as in LKO1 and LKO2 mice of the same age (Table 1). Thus, even a low concentration of Irs1 or Irs2 in the liver was sufficient to maintain normal circulating hormone and metabolite concentrations.

Next, we compared glucose tolerance and insulin sensitivity in 8-week-old mice. In comparison with DKO mice—which displayed severe glucose intolerance—DKO/1 and DKO/2 mice displayed intermediate glucose intolerance—DKO/1 mice being significantly better than DKO/2 mice (Fig. 4J and K). As previously shown (6), the DKO mice displayed severe insulin resistance during the i.p. insulin tolerance test (Fig. 4L and M). The DKO/1 and DKO/2 mice were significantly more sensitive to insulin than DKO mice; however, compared to the CNTR mice, the DKO/1 mice displayed a stronger response to

FIG. 1. Heat map of annotated reporter transcripts dependent upon Irs1 and Irs2 signaling for normal expression. Data are from Affymetrix GeneChips (MOE430 2) analysis. Expression was determined in chow-fed mice after 16 h of fasting with or without refeeding for 4 h. Transcript expression was determined in the fasting state, log2[fast]—or the change between fed and fasted states, log2[fed/fast]. The Pearson correlation coefficient was calculated versus CNTR samples together with the 95% CI.

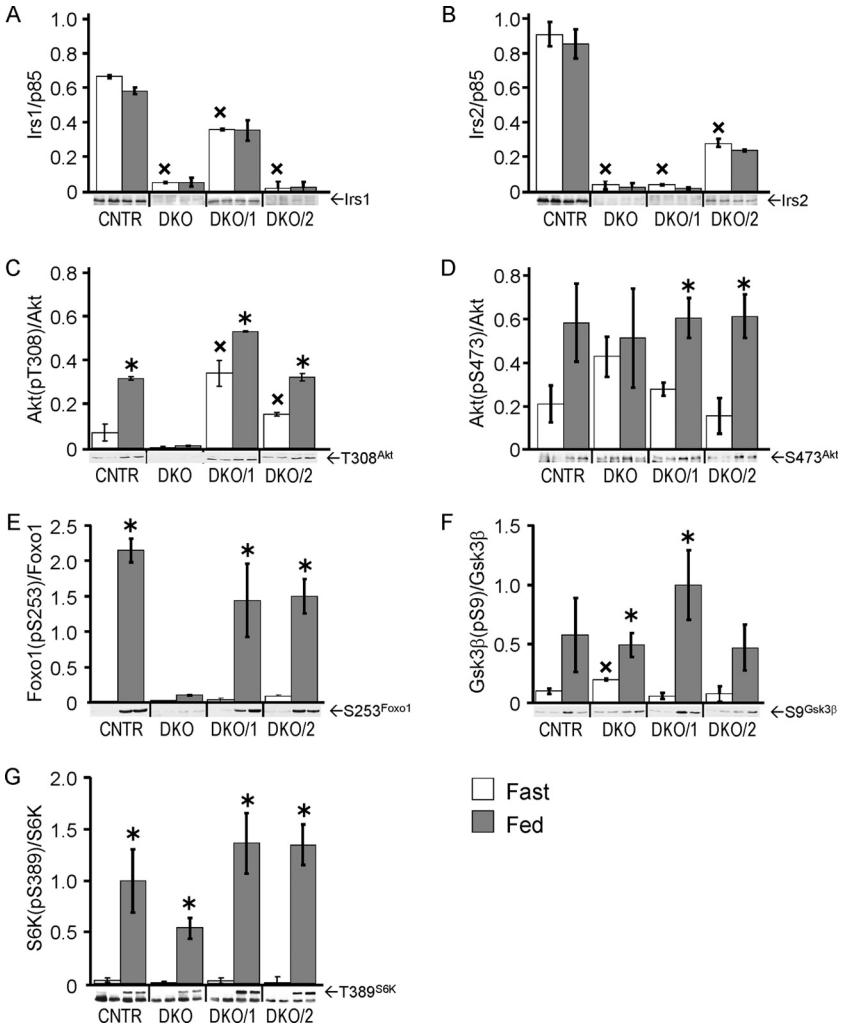

FIG. 2. Feeding-stimulated signaling in livers of DKO/1 and DKO/2 mice. Liver lysates from duplicate male mice fasted for 20 h or fed 4 h after the 20-h fast were separated by sodium dodecyl sulfate-polyacrylamide gel electrophoresis and immunoblotted with antibodies against Irs1 (A) or Irs2 (B) and p85, or total Akt, Foxo1, GSK3β, and S6K plus phospho-specific antibodies against Akt(T308) (C), Akt(S473) (D), Foxo1(S253) (E), GSK3β(Ser9) (F), and S6K(Thr389) (G). Bars represent averages ± SEM; the quantitated signals are shown beneath each graph. The intensity of each signal (numerator) was analyzed using a general linear model with genotype and fasted or fed state as factors and expression as a numerical covariate to correct the signal for variable expression. Statistical significance was set at $P < 0.05$ using the Bonferroni correction for multiple comparisons; ∗, $P < 0.05$ versus the same genotype and fasted state; ×, $P < 0.05$ versus CNTR fasted state.

insulin than did the DKO/2 mice (Fig. 4L and M). Thus, hepatic Irs1 mediated a stronger response than did Irs2 to injected glucose or insulin in mice.

Roles of hepatic Irs1 and Irs2 in direct and central control of hepatic glucose production. A hyperinsulinemic-euglycemic clamp was used to establish the relative contribution of Irs1 and Irs2 to systemic glucose homeostasis. During peripheral insulin infusion (2.5 mU kg^{-1} min^{-1}), the circulating glucose concentration in CNTR mice was maintained at 5 mM by infusing 275 μmol kg^{-1} min^{-1} glucose. The DKO mice required a much lower glucose infusion rate than did the CNTR mice, whereas the LKO1 or LKO2 mice were maintained at 5 mM by the infusion of 195 ± 20 and 183.8 ± 12 μmol kg^{-1} min^{-1} glucose, respectively. Thus, insulin sensitivity was partially impaired in the LKO1 and LKO2 mice but markedly dysregulated in the DKO mice (Fig. 5A).

Compared to the CNTR mice, basal hepatic glucose production was slightly—but not significantly—increased in fasted LKO1, LKO2, and DKO mice (Fig. 5B). The peripheral insulin infusion completely suppressed hepatic glucose production in the CNTR mice but had no effect upon LKO1, LKO2, or DKO mice (Fig. 5B). Thus, both Irs1 and Irs2 were required for the normal inhibition of hepatic glucose production during the hyperinsulinemic-euglycemic clamp. In comparison, the whole-body glucose disposal rate (Rd) decreased significantly in the DKO mice but increased slightly in LKO1 mice compared to the normal rate in the CNTR and LKO2 mice (Fig. 5C).

Hepatic glucose production can also be regulated by the indirect effects of insulin in the hypothalamus (8). In the brain, insulin suppresses hepatic glucose production via vagus nerve-mediated signals generated by insulin-stimulated closure of K-ATP channels (25, 30). To establish whether the central effect of insulin to inhibit hepatic glucose production also requires direct hepatic insulin signaling, we performed ICV in-

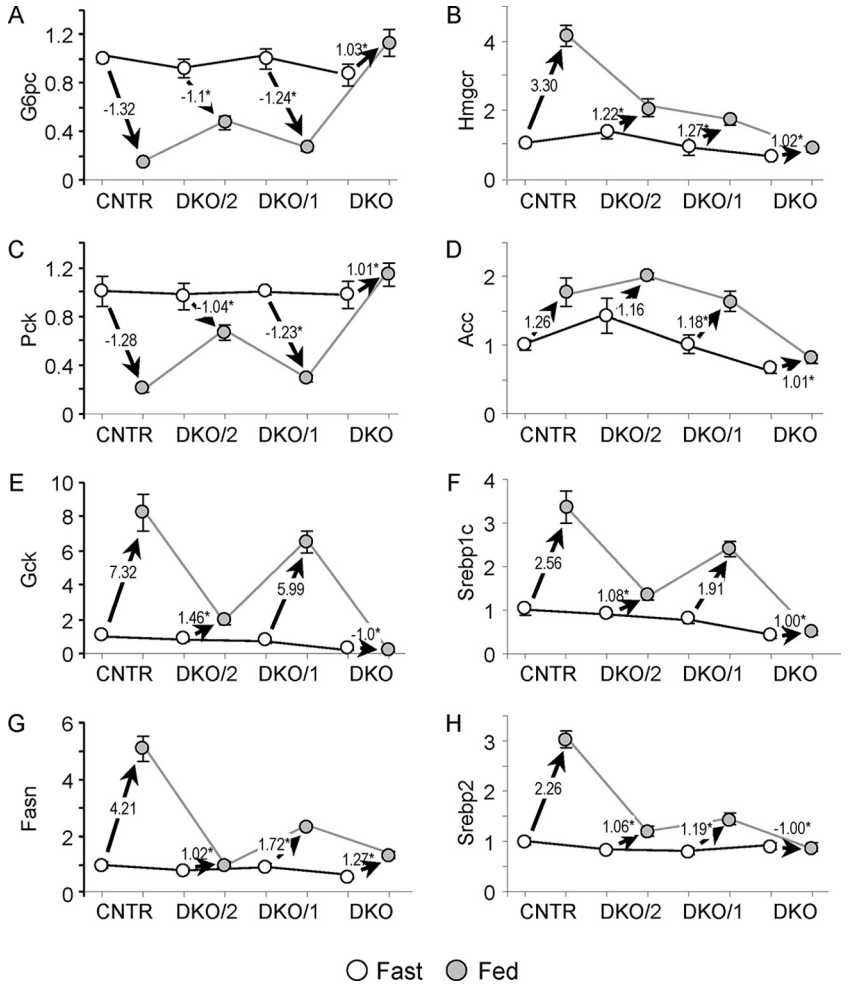

FIG. 3. Gene expression in fasted or fed livers from CNTR, DKO/2, DKO/1, and DKO mice maintained on the chow diet. Real-time PCR data for each gene were normalized against the corresponding fasted CNTR mouse values. Open circles represent expression in the fasted mice, and closed circles represent expression in the fed mice. Each graph is annotated with the value of the vector defining the expression change between fasted and fed mice ($n = 3$ mice per group). *, $P < 0.05$ versus feeding-stimulated change in CNTR mice.

sulin infusion while endogenous insulin secretion was inhibited by a pancreatic insulin clamp (30). Before initiating the ICV insulin infusion, the circulating glucose concentration was maintained at 5 mM in CNTR, LKO1, and LKO2 mice by infusing about 90 μmol kg^{-1} min^{-1} glucose; ~50% less glucose was required by the DKO mice (Fig. 5D). ICV insulin increased by twofold the rate of glucose infusion required to maintain the circulating glucose at 5 mM in CNTR, LKO1, and LKO2 mice (Fig. 5D); however, ICV insulin had no effect upon the DKO mice (Fig. 5D). Consistent with these results, ICV insulin significantly reduced hepatic glucose production in CNTR, LKO1, and LKO2 mice but had no effect upon the DKO mice (Fig. 5E). As expected, ICV insulin had no effect upon peripheral glucose disposal (Fig. 5F). Thus, a direct hepatic insulin signal through Irs1 or Irs2 was required to observe the inhibitory effect of ICV insulin upon hepatic glucose production.

Roless of hepatic Irs1 and Irs2 during nutrient stress. Obesity causes insulin resistance that can progress to diabetes. To establish the roles of Irs1 and Irs2 in response to this nutrient stress, we compared glucose homeostasis and feeding-stimulated signaling in LKO1 and LKO2 mice maintained for 12 weeks on a normal chow or HFD (Fig. 6). Chow-fed LKO1 and LKO2 mice showed a fasting metabolic profile indistinguishable from that of CNTR mice (Table 1). In contrast, all HFD-fed mice displayed elevated circulating glucose concentrations during the fasting state—though only the DKO mice were significantly hyperglycemic relative to the CNTR mice (Fig. 6A). During the HFD, postprandial blood glucose was elevated in the LKO1 and DKO mice, whereas that of LKO2 mice remained indistinguishable from that of CNTR mice (Fig. 6A). We previously showed that, when maintained on a regular chow diet, both LKO1 and LKO2 mice were normally sensitive to injected insulin, but LKO1 mice were mildly glucose intolerant (6). Consistent with these findings, HFD-fed LKO1 mice displayed severe glucose intolerance indistinguishable from that of DKO mice, while glucose tolerance of HFD-fed LKO2 mice was barely different from that of the CNTR mice and significantly better than that of the LKO1 mice (Fig. 6B and C). The HFD-fed LKO1 mice were also significantly less sen-

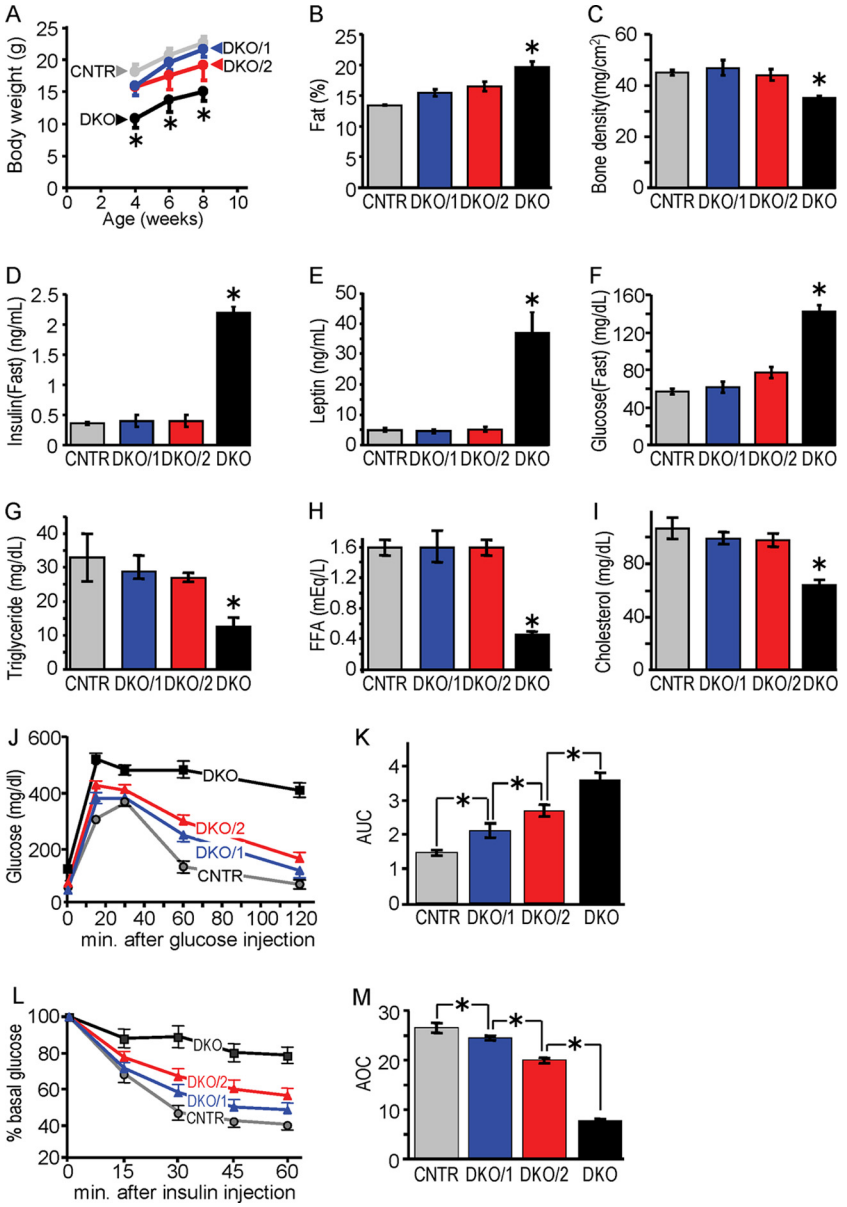

FIG. 4. Metabolic characterization of CNTR, DKO/1, DKO/2, and DKO mice: body weight (A), percent body fat (B), and bone mineral density determined by dual-energy X-ray absorptiometry at 8 weeks of age (C); plasma insulin (D), leptin (E), and blood glucose (F) concentrations, circulating triglyceride (G), free fatty acids (FFA) (H), and total cholesterol (I) in 8-week-old male mice. Values are averages ± SEM ($n = 8$ mice per group). Significance was calculated using a general linear model with genotype and fasting or feeding state as factors. *, $P < 0.05$ versus CNTR mice, using the Bonferroni correction for multiple comparisons. (J and K) Glucose tolerance tests performed at 8 weeks of age with male mice fasted for 16 h ($n = 6$/genotype); the results were summarized by determining the area under each curve (AUC), using Medcalc (v10). One-way analysis of variance (ANOVA) was used to compare the groups. *, $P < 0.05$. (L and M) Insulin tolerance tests performed with nonfasted 8-week-old male mice; the results were summarized by determining the area between 100% and each curve (AOC) using Medcalc. One-way ANOVA was used to compare the groups. *, $P < 0.05$.

sitive to injected insulin than were the LKO2 mice (Fig. 6D and E). Chow-fed LKO1 and LKO2 mice each exhibited normal fasting plasma insulin, triglyceride, and liver tissue triglyceride concentrations (Table 1). Among the HFD-fed mice, fasting plasma insulin concentrations in LKO1 and DKO mice were significantly elevated compared to those in the CNTR mice (Fig. 6F), whereas plasma and liver tissue triglyceride concentrations were significantly decreased (Fig. 6G and H); in contrast, each of these measurements was unchanged between HFD-fed LKO2 and CNTR mice (Fig. 6F to H). Thus, LKO2 mice exhibited responses to HFD feeding that were similar to those seen in CNTR mice, whereas LKO1 mice responded similarly to DKO mice.

Next, we investigated the effect of the HFD upon fasting and postprandial expression of several insulin-sensitive genes—including the G6pc, Pck, Gck, Fasn, Hmgcr, Acc, Srebp1c, and Srebp2 genes (Fig. 7). During fasting, gene expression was indistinguishable between CNTR, LKO1, and LKO2 mice, and

TABLE 1. Metabolic parameters for 8-week-old chow-fed mice[a]

Parameter	Value for indicated mice					
	CNTR	DKO	DKO/1	LKO2	DKO/2	LKO1
Blood glucose (mg/dl)	57 ± 3	142 ± 7[b]	61 ± 6	54 ± 7	77 ± 6	64 ± 6
Insulin (ng/ml)	0.36 ± 0.02	2.18 ± 0.15[b]	0.39 ± 0.07	0.32 ± 0.05	0.40 ± 0.12	0.38 ± 0.06
Leptin (ng/ml)	4.85 ± 0.58	36.68 ± 6.75[b]	4.63 ± 0.64	4.41 ± 1.2	5.17 ± 0.85	5.57 ± 1.88
Triglyceride (mg/dl)	33.1 ± 6.8	12.4 ± 0.6[b]	28.8 ± 4.7	29.1 ± 5.2	26.9 ± 1.6	30.3 ± 5.1
FFA (meq/liter)	1.63 ± 0.13	0.46 ± 0.05[b]	1.61 ± 0.19	1.45 ± 0.12	1.63 ± 0.05	1.39 ± 0.28
Cholesterol (mg/dl)	107 ± 8	64 ± 4[b]	99 ± 4		98 ± 5	
Albumin (g/dl)	3.01 ± 0.12	2.52 ± 0.16[b]	3.15 ± 0.26		3.10 ± 0.15	
Fed liver glycogen (mg/g)	55.2 ± 4.8	26.7 ± 1.8[b]	52.8 ± 4.2	54.6 ± 6.8	54 ± 2.4	57.3 ± 5.5
Liver triglyceride (mg/g)	44.2 ± 4.3	47.5 ± 4.8	49.6 ± 3.5	48.7 ± 6.5	40.38 ± 3.8	44.6 ± 4.7

[a] Unless noted otherwise in the text, measurements come from overnight-fasted mice. FFA, free fatty acid.
[b] $P < 0.05$ versus CNTR mice.

postprandial gene expression in HFD-fed CNTR mice changed in the expected direction; that is, the G6pc and Pck genes decreased upon feeding, whereas the Hmgcr, Acc, Gck, Srebp1c, Srebp2, and Fasn genes increased upon feeding (Fig. 7A to H). However, compared to chow-fed mice, the effect of feeding upon Gck was reduced about threefold in the HFD-fed CNTR mice (compare Fig. 7E and 3E). The LKO1 liver—which retains only Irs2—displayed markedly impaired postprandial changes in expression of the G6pc, Pck, Gck, Fasn, Hmgcr, and Srebp2 genes (Fig. 7A, C, E, G, B, and H). In contrast, postprandial gene expression in the LKO2 liver resembled more closely the expression in the CNTR liver. The Acc and Srebp1c genes were notable exceptions, as these genes dysregulated similarly in LKO1 and LKO2 livers (Fig. 7D and F). Overall, however, Irs1 played a more dominant role in postprandial liver gene expression during HFD feeding.

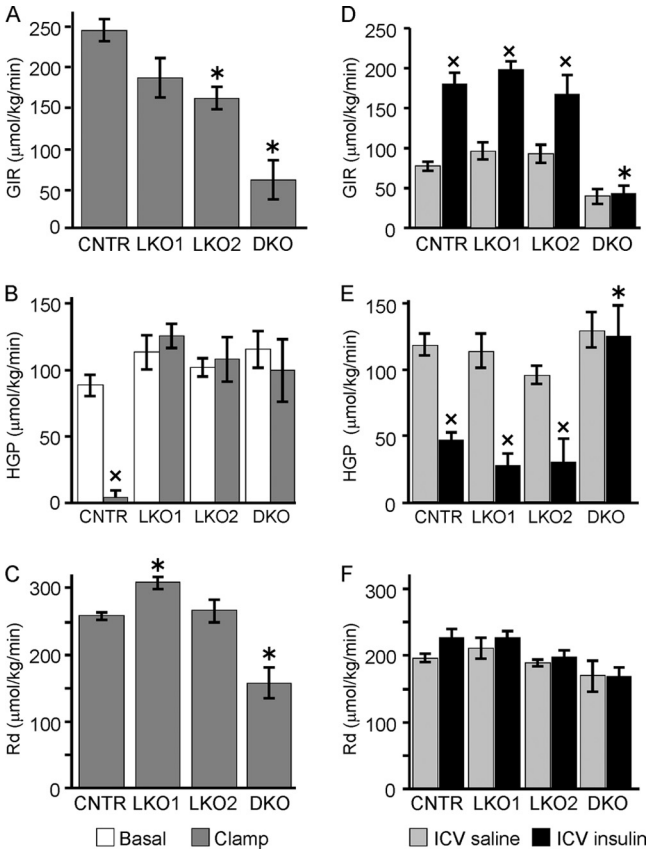

FIG. 5. Hyperinsulinemic-euglycemic clamp (A to C) and ICV clamp analysis (D to F) in CNTR, LKO1, LKO2, and DKO mice. Graphs show the averages ± SEM for each parameter obtained (n = 6 mice per group) as follows. Peripheral glucose infusion rate (GIR) (A and D); hepatic glucose production (HGP) (B and E); peripheral glucose disposal (Rd) (C and F). Comparisons were made using a general linear model with genotype and insulin infusion as factors, and significant differences were taken at $P < 0.05$, using the Bonferroni correction for multiple comparisons. *, $P < 0.05$ versus CNTR mice; ×, $P < 0.05$ versus basal (B) or saline infusion (D to F).

Finally, we investigated tyrosine phosphorylation of Irs1 and Irs2 and several downstream responses in the liver of HFD-fed mice that were fasted (20 h) or fasted for 20 h and fed for 4 h. Irs1 protein was detected equally by immunoblotting in fasted and fed CNTR and LKO2 livers, and Irs2 was detected equally in fasted and fed CNTR and LKO1 livers (data not shown). Both Irs1 and Irs2 were tyrosine phosphorylated at the end of the fast (Fig. 8A to D). Tyrosine phosphorylation of Irs1 increased between 1.5- and 2-fold, after feeding in the livers of CNTR or LKO2 mice maintained on HFD or chow (Fig. 8A and B). However, Irs2 tyrosine phosphorylation was not significantly stimulated by 4 h of feeding in HFD-fed CNTR and LKO1 mouse livers owing to elevated basal phosphorylation (Fig. 8C). It was also barely increased following feeding in the livers of chow-fed CNTR and LKO1 mice (Fig. 8D). Regardless, Akt(T308) phosphorylation at 4 h after feeding was equivalently stimulated in HFD-fed CNTR, LKO1, and LKO2 mice, whereas it was barely detected in fasted or fed DKO mice (Fig. 8E).

Like Akt, aPKC is activated by the PI3K cascade; however, aPKC is coupled exclusively to the Irs2 branch of the insulin signaling cascade (34, 39). Regardless of the diet, feeding stimulated aPKC activity about twofold in the livers of CNTR and LKO1 mice but had no effect upon aPKC activity in the livers of LKO2 or DKO mice (Fig. 8F and G). Recent studies suggest that Akt is primarily responsible for suppressing expression of the G6pc and Pck genes, whereas aPKC preferentially increases the expression of lipogenic genes, such as Srebp1c (39). However, 4 h of feeding decreased expression of the Pck gene by at least 50% in CNTR and LKO2 livers—but not in the LKO1 liver—even though feeding-stimulated Akt(T308) phosphorylation was the same at this time point (Fig. 8E). Moreover, feeding substantially increased expression of the Gck,

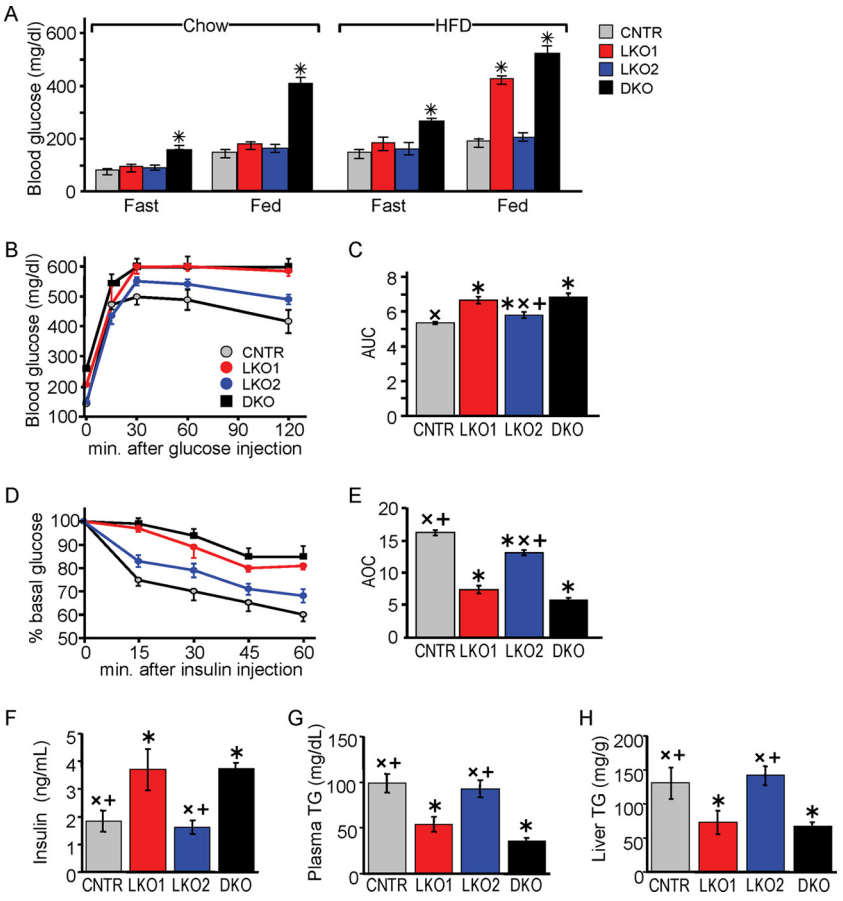

FIG. 6. Nutrient homeostasis in HFD-fed LKO1 and LKO2 mice. (A) Blood glucose concentrations (average ± SEM; $n = 6$) determined after 16 h fast with or without 4 h of refeeding in 4-month-old male CNTR, LKO1, LKO2, and DKO mice fed chow or an HFD. (B and C) Glucose tolerance test results for 4-month-old overnight-fasted mice ($n = 6$ per group); the results were summarized by determining the area under each curve (AUC), using Medcalc (v10). (D and E) Insulin tolerance test results for nonfasted 4-month-old male mice ($n = 6$); the results were summarized as the average area between 100% and each curve (AOC), determined using Medcalc. Fasting plasma insulin and triglyceride (TG) concentration (F and G), and liver triglyceride content (H) determined after 12 weeks of HFD feeding ($n = 6$). One-way ANOVA was used to compare the groups. *, $P < 0.05$ versus CNTR mice; ×, $P < 0.05$ versus DKO mice; +, $P < 0.05$ versus LKO1 mice.

Fasn, and Hmgcr lipogenic genes in CNTR and LKO2 mice—but not in LKO1 mice in which aPKC activation was normal (Fig. 7). Thus, after 4 h of feeding, maintenance of normal hepatic gene expression was better correlated with Irs1 expression and tyrosine phosphorylation than with either Akt or aPKC activation.

DISCUSSION

Our results identify Irs1 as the principal mediator of hepatic insulin action especially during nutrient excess imposed by weeks of HFD feeding. Without hepatic Irs1 (LKO1 mice), fasting and postprandial gene expression is significantly dysregulated compared to CNTR mice or mice without Irs2 (LKO2 mice). Indeed, even the low concentration of Irs1 in DKO/1 mice is sufficient to maintain nearly normal gene expression, fasting glucose concentrations, and postprandial glucose tolerance. When fed an HFD, LKO1 mice—which retain normal Irs2 expression—develop severe glucose intolerance and diabetes that are indistinguishable from those seen in mice completely lacking Irs1 and Irs2 (DKO mice). Although LKO2 mice also develop abnormal glucose tolerance on the HFD, they are indistinguishable from CNTR mice—and significantly better than LKO1 and DKO mice. We conclude that hepatic Irs1 is a principal mediator of the transition between fasting and postprandial glucose homeostasis, especially during nutrient excess.

Previous reports point to Irs2 as the critical mediator of hepatic insulin action. Hepatocytes with low insulin receptor concentrations retain significant Irs1 phosphorylation during insulin stimulation, while typical biological insulin responses and Irs2 phosphorylation fail (33). Neonatal $Irs2^{-/-}$ hepatocyte cell lines retain insulin-stimulated Irs1 tyrosine phosphorylation, while insulin weakly activates PI3K, Akt, or aPKC and weakly inhibits Gsk3α/β or Foxo1 (41). Moreover, recent work suggests that Irs2 is an important mediator of fasting insulin action in adult murine hepatocytes, at least in part because Irs2 mRNA and protein concentrations increase during the fasting state (16). Presumably, Irs2 amplifies the hepatic insulin signal generated by a low fasting concentration of insulin—which

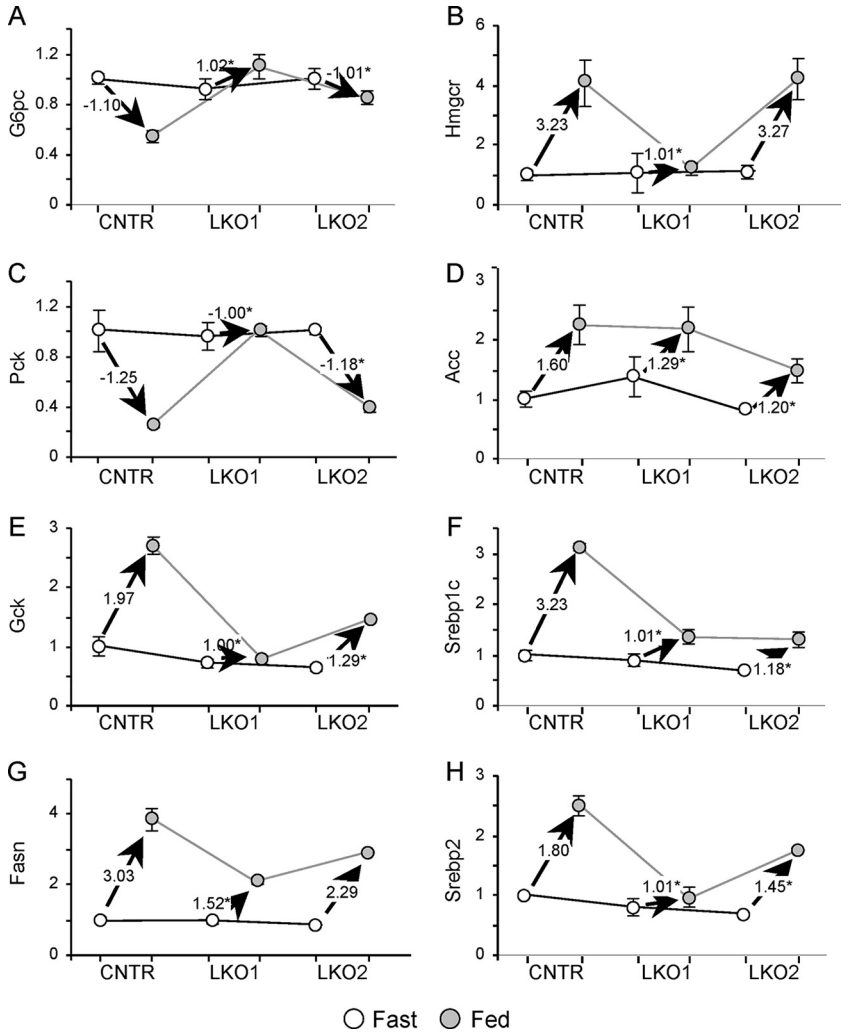

FIG. 7. Gene expression in fasted or fed livers from 4-month-old CNTR, LKO1, and LKO2 mice maintained on the HFD. Real-time PCR data for each gene were normalized against the corresponding fasted CNTR mouse values. Open circles represent expression in the fasted mice, and closed circles represent expression in the fed mice. Each graph is annotated with the value of the vector defining the expression change between fasted and fed mice ($n = 3$ mice per group). *, $P < 0.05$ versus feeding-stimulated change in CNTR mice.

might attenuate the counterregulatory effects of glucagon and promote a rapid and complete response to insulin immediately upon food intake (16).

Regardless, genetic deletion of Irs1 or Irs2 in hepatocytes suggests that Irs1 is a dominant mediator of feeding-regulated hepatic gene expression. The concentrations of reporter transcripts—which depend upon insulin signaling for the fasting→postprandial transition—are slightly dysregulated in the DKO/1 liver but severely dysregulated in the DKO/2 liver, the distinct regulation being especially significant for the G6pc and Pck gluconeogenic genes and the Gck, Fasn, and Srebp1c lipogenic genes. This difference corresponds to the finding that DKO/2 mice—or LKO1 mice shown previously (6)—display dysregulated glucose and insulin tolerance. Thus, in our experimental setting, hepatic Irs1 has a dominant role in coordinating hepatic gene expression and glucose homeostasis.

Consumption of the HFD causes glucose intolerance in all of our experimental mice. Regardless, gene expression and glucose tolerance in LKO2 and CNTR mice are nearly indistinguishable, suggesting that Irs1 is largely responsible for maintaining hepatic insulin action during chronic nutrient excess. This conclusion is strengthened by the finding that HFD-fed LKO1 mice are indistinguishable from DKO mice, suggesting that hepatic Irs2 alone largely fails during chronic nutrient excess. These results are generally consistent with the previous conclusion that the Irs1 cascade predominates in hepatocytes during the postprandial state (16). Nutrient excess imposed by weeks of HFD feeding might place the mouse in a chronic postprandial state that preferentially inactivates Irs2, leaving LKO1 mice with an insufficient insulin response that resembles the DKO mice. Conventional signaling experiments show that postprandial phosphorylation of Akt(T308) or Foxo1(S253)—which is absent in DKO liver—is largely retained in DKO/1 or DKO/2 liver. In contrast, the phosphorylation of Akt(S473), Gsk3β(S9), and S6K(pS389) does not absolutely require Irs1 or Irs2, although the increase from the fasting to fed state occurs more normally in the DKO/1 or DKO/2 mice. The basal phosphorylation of Akt(T308) is high in the DKO/1 liver but is

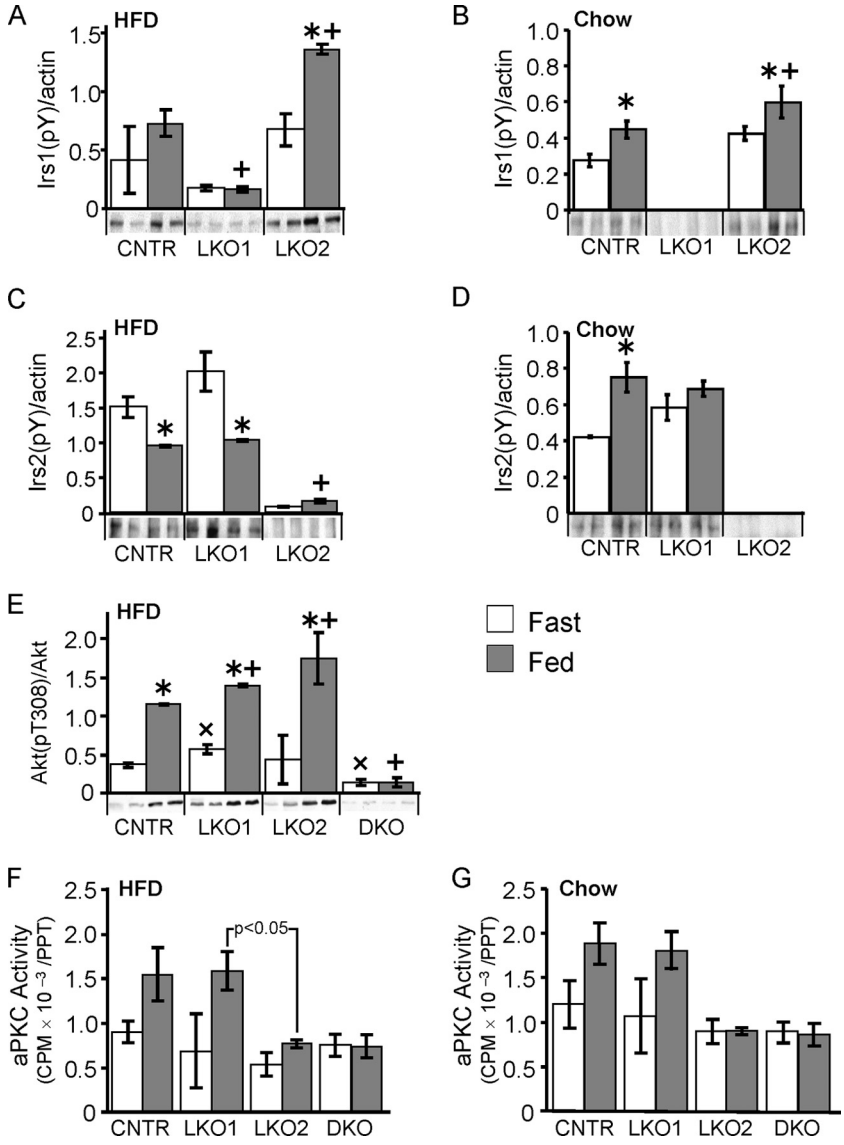

FIG. 8. Feeding-stimulated signaling in livers of HFD- and chow-fed LKO1 and LKO2 mice. Liver tissues from duplicate male mice fasted for 20 h or fed for 4 h after the 20-h fast were analyzed by immunoprecipitation and/or immunoblotting. Tyrosine phosphorylation (pY) of Irs1 (A and B) and Irs2 (C and D) was determined by immunoprecipitation and immunoblotting with antiphosphotyrosine antibody. Feeding-stimulated phosphorylation of Akt(T308) (E) and aPKC activity ($n = 3$ per group) (F and G). Bars represent averages ± SEM; the quantitated signals are shown beneath each graph. The intensity of each signal (numerator) was analyzed using a general linear model, with genotype and fasted or fed state as factors and expression (or expression of actin for pY) as a numerical covariate to correct the signal for variable expression. Statistical significance was set at $P < 0.05$ using the Bonferroni correction for multiple comparisons; ∗, $P < 0.05$ versus genotype and fasted state; ×, $P < 0.05$ versus CNTR fasted state; +, $P < 0.05$ versus CNTR fed state.

further stimulated by feeding, which might explain the better glucose tolerance observed for DKO/1 mice. Gsk3β(S9) phosphorylation is stronger in the DKO/1 mice than in the DKO/2 mice, whereas Foxo1(S253) and S6K(pS389) phosphorylation is indistinguishable. In contrast, postprandial aPKC activity increases normally in CNTR and LKO1 mice but not in fed LKO2 or DKO mice, consistent with a specific link to Irs2-mediated PI3K signaling (7, 39). Additional work is needed to understand how Irs2 couples specifically to aPKC and to identify the Irs1/2-independent mechanisms that promote phosphorylation of Akt(S473), Gsk3β(S9), and S6K(pS389) in fed DKO mice.

After prolonged maintenance on an HFD, feeding still stimulates Irs1 tyrosine phosphorylation in CNTR and LKO2 mice, whereas it fails to stimulate Irs2 phosphorylation in CNTR and LKO1 mice. While Akt(T308) phosphorylation is stimulated in either case, this seems slightly stronger in LKO2 mice than in LKO1 mice. Consistent with chow-fed mice, postprandial aPKC activation proceeds normally in the LKO1 liver but fails in the LKO2 liver. Earlier data suggest that aPKC—especially PKCλ that is most abundant in the liver—mainly promotes SREBP-1c expression and triglyceride synthesis (20, 39), whereas Akt suppresses gluconeogenic gene expression via Foxo1 (12, 21, 36, 45, 47). However, constitutively active Akt

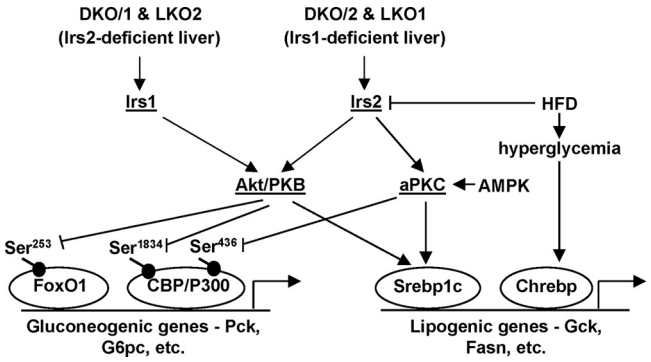

FIG. 9. Model of regulation of hepatic gene expression and metabolism by Irs1 and Irs2 via Akt and aPKC. AMPK, AMP-activated protein kinase; →, activation; ⊣, inhibition.

also increases Srebp1c gene expression and induces marked hypertriglyceridemia (26). Likewise, activation of aPKC by insulin or by metformin via AMPK phosphorylates CBP/p300 at Ser436 to disrupt association with the CREB-TORC2 complex, a key component in the control of gluconeogenic gene expression (13a). Moreover, phosphorylation of CBP/p300 at Ser1834 by Akt disrupts association of CBP with C/EBPβ, inhibiting hepatic gene expression (10). Thus, Akt and aPKC both contribute substantially to the control of gluconeogenic and lipogenic gene expression, as summarized in Fig. 9.

Our studies indicate that postprandial expression of the Gck, Fasn, Srebp1c and Srebp2 genes are, in general, slightly reduced in the DKO/1 or LKO2 liver but substantially reduced in the DKO/2 or LKO1 liver, demonstrating the primary importance of Irs1 for the control of triglyceride synthetic gene expression in this system. However, glucose itself can promote expression of lipogenic genes, including the Fasn and Acc genes, via an insulin-independent pathway involving Chrebp (14) (Fig. 9). This pathway is likely to have augmented expression of these genes in hyperglycemic chow-fed DKO and HFD-fed LKO1 mice (Fig. 9). Nevertheless, circulating triglyceride concentrations in these mice were significantly lower than those in controls.

Although the HFD clearly distinguishes hepatic Irs1 signaling from Irs2 signaling, the moderate cost of deleting hepatic Irs2 in chow-fed mice can be detected by glucose and insulin tolerance tests. A joint requirement for Irs1 and Irs2 is detected by the hyperinsulinemic-euglycemic clamp conducted with a low insulin infusion rate (2.5 mU kg^{-1} min^{-1}), which strongly suppresses hepatic glucose production in CNTR mice, but not in LKO1 or LKO2 mice. Using a higher insulin infusion rate (5.0 mU kg^{-1} min^{-1} for their LKO1 mice, or 7.5 mU kg^{-1} min^{-1} for their LKO2 mice), Kubota et al. (16) found that glucose production is inhibited more strongly in LKO1 liver than in LKO2 liver, suggesting that Irs2 is critical to suppress glucose production. A conservative synthesis of these results is that both Irs1 and Irs2 are required for the most sensitive hepatic response and Irs1 is more important during nutrient excess or when insulin is limiting.

In addition to directly suppressing gluconeogenesis through Irs1- and Irs2-mediated signaling in hepatocytes, insulin also has indirect effects upon hepatic glucose production through action in the hypothalamus (30). Several reports suggest that hypothalamic insulin action is mediated via Irs2 and transmitted to the liver through the vagus nerve (24, 25, 29, 30). Whether this central effect of insulin upon the liver is sufficient to suppress glucose production is controversial (3). However, our results indicate that direct hepatic insulin signaling through either Irs1 or Irs2 is essential for the central effect of insulin, because glucose production is not inhibited in fasting DKO mice by central insulin infusion. Unlike peripheral insulin infusion, which requires both Irs1 and Irs2 for full effect, centrally infused insulin requires either hepatic Irs1 or Irs2. Our previous work suggests that the normal transition between the fasting and postprandial states depends upon the inactivation of hepatic Foxo1 by insulin, which is nearly impossible to achieve in DKO mice (6). In comparison, insulin-resistant DKO mice without hepatic Foxo1 display nearly normal fasting and postprandial glucose homeostasis. Thus, inactivation of Foxo1—or the deletion of Foxo1 in DKO mice—might be required for the hepatic response to the central insulin. Direct experimentation of the triple knockout mice is needed to test this hypothesis.

The acute suppression of both Irs1 and Irs2 by at least 80% in the liver, using shRNA, produces effects upon glucose homeostasis that are similar to those in DKO/1, DKO/2, and DKO mice (40). However, lipid homeostasis is different in these experimental models; the residual Irs signal in DKO/1 and DKO/2 mice is composed of either Irs1 or Irs2, respectively, while the residual Irs signal in shRNA-treated mice is composed of mixtures of Irs1 and Irs2. In both models, gluconeogenic gene expression is nearly normal in liver retaining Irs1 but abnormal in liver in which Irs1 is reduced or absent. A difference is that Srebp1c and Fasn mRNAs increase in liver treated with shRNA against Irs2 or both Irs1 and Irs2, leading to the conclusion that Irs2 is the principal regulator of hepatic lipogenesis (40). Regardless, the transition of these genes from the fasted state to the postprandial state is nearly normal in DKO/1 mice but reduced significantly in DKO/2 and DKO mice; a similar pattern emerges in the LKO1 and LKO2 mice fed an HFD. Thus, our results support the hypothesis that Irs1 is the dominant regulator of hepatic gene expression controlling lipogenesis—probably because it mediates the long-term effects of insulin needed to induce Srebp1c.

In summary, a low concentration of Irs1 or Irs2 can mediate the fasting and postprandial hepatic insulin response to feeding under conditions of ordinary nutrition provided by chow diets. However, a dominant role for Irs1 is seen during nutrient excess, in conjunction with reduced feeding-stimulated signaling by Irs2. While persistent Irs1 signaling better controls hepatic glucose homeostasis, it also promotes lipogenesis that can lead to hepatic steatosis. Thus, characteristics of dyslipidemia were most prominent in the hyperinsulinemic shRNA-treated mice—which retain low concentrations of Irs1 and Irs2—suggesting that hyperinsulinemia in the presence of diminished Irs1/2 signaling might promote steatosis (40). Although our DKO mice are also hyperinsulinemic, they lack Irs1 and Irs2, so the chronic effect upon lipogenesis is largely absent (13). Consistent with the study by Kubota et al. (16), Irs2 appears to be important in the early postprandial period to augment the initial response to insulin—not as the exclusive suppressor of hepatic glucose production—but to reduce the requirement for

long-term insulin action that can lead to Irs1-mediated lipid production.

ACKNOWLEDGMENTS

This work was funded by the Howard Hughes Medical Institute and U.S. National Institutes of Health grants DK038712 and DK055326. S.G. is supported by an American Diabetes Association Junior Faculty grant (7-07-JF-27).

REFERENCES

1. **Araki, E., M. A. Lipes, M. E. Patti, J. C. Bruning, B. Haag III, R. S. Johnson, and C. R. Kahn.** 1994. Alternative pathway of insulin signalling in mice with targeted disruption of the IRS-1 gene. Nature **372:**186–190.
2. **Baumann, C. A., V. Ribon, M. Kanzaki, D. C. Thurmond, S. Mora, S. Shigematsu, P. E. Bickel, J. E. Pessin, and A. R. Saltiel.** 2000. CAP defines a second signalling pathway required for insulin-stimulated glucose transport. Nature **407:**202–207.
3. **Buettner, C., R. Patel, E. D. Muse, S. Bhanot, B. P. Monia, R. McKay, S. Obici, and L. Rossetti.** 2005. Severe impairment in liver insulin signaling fails to alter hepatic insulin action in conscious mice. J. Clin. Investig. **115:**1306–1313.
4. **Chiang, S. H., C. A. Baumann, M. Kanzaki, D. C. Thurmond, R. T. Watson, C. L. Neudauer, I. G. Macara, J. E. Pessin, and A. R. Saltiel.** 2001. Insulin-stimulated GLUT4 translocation requires the CAP-dependent activation of TC10. Nature **410:**944–948.
5. **Dong, X., S. Park, X. Lin, K. Copps, X. Yi, and M. F. White.** 2006. Irs1 and Irs2 signaling is essential for hepatic glucose homeostasis and systemic growth. J. Clin. Investig. **116:**101–114.
6. **Dong, X. C., K. D. Copps, S. Guo, Y. Li, R. Kollipara, R. A. DePinho, and M. F. White.** 2008. Inactivation of hepatic Foxo1 by insulin signaling is required for adaptive nutrient homeostasis and endocrine growth regulation. Cell Metab. **8:**65–76.
7. **Farese, R. V., M. P. Sajan, and M. L. Standaert.** 2005. Atypical protein kinase C in insulin action and insulin resistance. Biochem. Soc. Trans. **33:**350–353.
8. **Girard, J.** 2006. The inhibitory effects of insulin on hepatic glucose production are both direct and indirect. Diabetes **55**(Suppl. 2)**:**S65–S69.
9. **Gribble, F. M.** 2005. Metabolism: a higher power for insulin. Nature **434:**965–966.
10. **Guo, S., S. B. Cichy, X. He, Q. Yang, M. Ragland, A. K. Ghosh, P. F. Johnson, and T. G. Unterman.** 2001. Insulin suppresses transactivation by CAAT/enhancer-binding proteins beta (C/EBPbeta). Signaling to p300/CREB-binding protein by protein kinase B disrupts interaction with the major activation domain of C/EBPbeta. J. Biol. Chem. **276:**8516–8523.
11. **Guo, S., S. L. Dunn, and M. F. White.** 2006. The reciprocal stability of FOXO1 and IRS2 creates a regulatory circuit that controls insulin signaling. Mol. Endocrinol. **20:**3389–3399.
12. **Guo, S., G. Rena, S. Cichy, X. He, P. Cohen, and T. Unterman.** 1999. Phosphorylation of serine 256 by protein kinase B disrupts transactivation by FKHR and mediates effects of insulin on insulin-like growth factor-binding protein-1 promoter activity through a conserved insulin response sequence. J. Biol. Chem. **274:**17184–17192.
13. **Haeusler, R. A., and D. Accili.** 2008. The double life of Irs. Cell Metab. **8:**7–9.

13a. **He, L., A. Sabet, S. Djedjos, R. Meller, X. Sun, M. A. Hussain, S. Radovick, and F. E. Wondisford.** 2009. Metformin and insulin suppress hepatic gluconeogenesis through phosphorylation of CREB binding protein. Cell **137:**635–646.

14. **Ishii, S., K. Iizuka, B. C. Miller, and K. Uyeda.** 2004. Carbohydrate response element binding protein directly promotes lipogenic enzyme gene transcription. Proc. Natl. Acad. Sci. USA **101:**15597–15602.
15. **Kotani, K., P. Wilden, and T. S. Pillay.** 1998. SH2-Balpha is an insulin-receptor adapter protein and substrate that interacts with the activation loop of the insulin-receptor kinase. Biochem. J. **335:**103–109.
16. **Kubota, N., T. Kubota, S. Itoh, H. Kumagai, H. Kozono, I. Takamoto, T. Mineyama, H. Ogata, K. Tokuyama, M. Ohsugi, T. Sasako, M. Moroi, K. Sugi, S. Kakuta, Y. Iwakura, T. Noda, S. Ohnishi, R. Nagai, K. Tobe, Y. Terauchi, K. Ueki, and T. Kadowaki.** 2008. Dynamic functional relay between insulin receptor substrate 1 and 2 in hepatic insulin signaling during fasting and feeding. Cell Metab. **8:**49–64.
17. **Lin, X., A. Taguchi, S. Park, J. A. Kushner, F. Li, Y. Li, and M. F. White.** 2004. Dysregulation of insulin receptor substrate 2 in beta cells and brain causes obesity and diabetes. J. Clin. Investig. **114:**908–916.
18. Reference deleted.
19. **Lock, P., F. Casagranda, and A. R. Dunn.** 1999. Independent SH2-binding sites mediate interaction of Dok-related protein with RasGTPase-activating protein and Nck. J. Biol. Chem. **274:**22775–22784.
20. **Matsumoto, M., W. Ogawa, K. Akimoto, H. Inoue, K. Miyake, K. Furukawa, Y. Hayashi, H. Iguchi, Y. Matsuki, R. Hiramatsu, H. Shimano, N. Yamada, S. Ohno, M. Kasuga, and T. Noda.** 2003. PKClambda in liver mediates insulin-induced SREBP-1c expression and determines both hepatic lipid content and overall insulin sensitivity. J. Clin. Investig. **112:**935–944.
21. **Matsumoto, M., A. Pocai, L. Rossetti, R. A. DePinho, and D. Accili.** 2007. Impaired regulation of hepatic glucose production in mice lacking the forkhead transcription factor foxo1 in liver. Cell Metab. **6:**208–216.
22. **Mora, A., C. Lipina, F. Tronche, C. Sutherland, and D. R. Alessi.** 2005. Deficiency of PDK1 in liver results in glucose intolerance, impairment of insulin-regulated gene expression and liver failure. Biochem. J. **385:**639–648.
23. **Noguchi, T., T. Matozaki, K. Inagaki, M. Tsuda, K. Fukunaga, Y. Kitamura, T. Kitamura, K. Shii, Y. Yamanashi, and M. Kasuga.** 1999. Tyrosine phosphorylation of p62(Dok) induced by cell adhesion and insulin: possible role in cell migration. EMBO J. **18:**1748–1760.
24. **Obici, S., Z. Feng, G. Karkanias, D. G. Baskin, and L. Rossetti.** 2002. Decreasing hypothalamic insulin receptors causes hyperphagia and insulin resistance in rats. Nat. Neurosci. **5:**566–572.
25. **Obici, S., B. B. Zhang, G. Karkanias, and L. Rossetti.** 2002. Hypothalamic insulin signaling is required for inhibition of glucose production. Nat. Med. **8:**1376–1382.
26. **Ono, H., H. Shimano, H. Katagiri, N. Yahagi, H. Sakoda, Y. Onishi, M. Anai, T. Ogihara, M. Fujishiro, A. Y. Viana, Y. Fukushima, M. Abe, N. Shojima, M. Kikuchi, N. Yamada, Y. Oka, and T. Asano.** 2003. Hepatic Akt activation induces marked hypoglycemia, hepatomegaly, and hypertriglyceridemia with sterol regulatory element binding protein involvement. Diabetes **52:**2905–2913.
27. **Pawson, T., and J. D. Scott.** 1997. Signaling through scaffold, anchoring, and adaptor proteins. Science **278:**2075–2080.
28. **Plum, L., B. F. Belgardt, and J. C. Bruning.** 2006. Central insulin action in energy and glucose homeostasis. J. Clin. Investig. **116:**1761–1766.
29. **Pocai, A., T. K. Lam, R. Gutierrez-Juarez, S. Obici, G. J. Schwartz, J. Bryan, L. Huilar-Bryan, and L. Rossetti.** 2005. Hypothalamic K(ATP) channels control hepatic glucose production. Nature **434:**1026–1031.
30. **Pocai, A., S. Obici, G. J. Schwartz, and L. Rossetti.** 2005. A brain-liver circuit regulates glucose homeostasis. Cell Metab. **1:**53–61.
31. **Postic, C., and M. A. Magnuson.** 2000. DNA excision in liver by an albumin-Cre transgene occurs progressively with age. Genesis **26:**149–150.
32. **Previs, S. F., D. J. Withers, J. M. Ren, M. F. White, and G. I. Shulman.** 2000. Contrasting effects of IRS-1 versus IRS-2 gene disruption on carbohydrate and lipid metabolism in vivo. J. Biol. Chem. **275:**38990–38994.
33. **Rother, K. I., Y. Imai, M. Caruso, F. Beguinot, P. Formisano, and D. Accili.** 1998. Evidence that IRS-2 phosphorylation is required for insulin action in hepatocytes. J. Biol. Chem. **273:**17491–17497.
34. **Sajan, M. P., M. L. Standaert, A. Miura, C. R. Kahn, and R. V. Farese.** 2004. Tissue-specific differences in activation of atypical protein kinase C and protein kinase B in muscle, liver and adipocytes of insulin receptor substrate-1 knockout mice. Mol. Endocrinol. **18:**2513–2521.
35. **Saltiel, A. R., and C. R. Kahn.** 2001. Insulin signalling and the regulation of glucose and lipid metabolism. Nature **414:**799–806.
36. **Schmoll, D., K. S. Walker, D. R. Alessi, R. Grempler, A. Burchell, S. Guo, R. Walther, and T. G. Unterman.** 2000. Regulation of glucose-6-phosphatase gene expression by protein kinase Balpha and the forkhead transcription factor FKHR. Evidence for insulin response unit-dependent and -independent effects of insulin on promoter activity. J. Biol. Chem. **275:**36324–36333.
37. **Standaert, M. L., M. P. Sajan, A. Miura, Y. Kanoh, H. C. Chen, R. V. Farese, Jr., and R. V. Farese.** 2004. Insulin-induced activation of atypical protein kinase C, but not protein kinase B, is maintained in diabetic (ob/ob and Goto-Kakazaki) liver. Contrasting insulin signaling patterns in liver versus muscle define phenotypes of type 2 diabetic and high fat-induced insulin-resistant states. J. Biol. Chem. **279:**24929–24934.
38. **Tamemoto, H., T. Kadowaki, K. Tobe, T. Yagi, H. Sakura, T. Hayakawa, Y. Terauchi, K. Ueki, Y. Kaburagi, S. Satoh, H. Sekihara, S. Yoshioka, H. Horikoshi, Y. Furuta, Y. Ikawa, M. Kasuga, Y. Yazaki, and S. Aizawa.** 1994. Insulin resistance and growth retardation in mice lacking insulin receptor substrate-1. Nature **372:**182–186.
39. **Taniguchi, C. M., T. Kondo, M. Sajan, J. Luo, R. Bronson, T. Asano, R. Farese, L. C. Cantley, and C. R. Kahn.** 2006. Divergent regulation of hepatic glucose and lipid metabolism by phosphoinositide 3-kinase via Akt and PKClambda/zeta. Cell Metab. **3:**343–353.
40. **Taniguchi, C. M., K. Ueki, and C. R. Kahn.** 2005. Complementary roles of IRS-1 and IRS-2 in the hepatic regulation of metabolism. J. Clin. Investig. **115:**718–727.
41. **Valverde, A. M., D. J. Burks, I. Fabregat, T. L. Fisher, J. Carretero, M. F. White, and M. Benito.** 2003. Molecular mechanisms of insulin resistance in IRS-2-deficient hepatocytes. Diabetes **52:**2239–2248.
42. **White, M. F.** 2003. Insulin signaling in health and disease. Science **302:**1710–1711.
43. **White, M. F., and C. R. Kahn.** 1994. The insulin signaling system. J. Biol. Chem. **269:**1–4.
44. **Withers, D. J., J. S. Gutierrez, H. Towery, D. J. Burks, J. M. Ren, S. Previs, Y. Zhang, D. Bernal, S. Pons, G. I. Shulman, S. Bonner-Weir, and M. F.**

White. 1998. Disruption of IRS-2 causes type 2 diabetes in mice. Nature **391:**900–904.

45. **Yeagley, D., S. Guo, T. Unterman, and P. G. Quinn.** 2001. Gene- and activation-specific mechanisms for insulin inhibition of basal and glucocorticoid-induced insulin-like growth factor binding protein-1 and phosphoenolpyruvate carboxykinase transcription. Roles of forkhead and insulin response sequences. J. Biol. Chem. **276:**33705–33710.
46. **Yenush, L., and M. F. White.** 1997. The IRS-signaling system during insulin and cytokine action. Bioessays **19:**491–500.
47. **Zhang, W., S. Patil, B. Chauhan, S. Guo, D. R. Powell, J. Le, A. Klotsas, R. Matika, X. Xiao, R. Franks, K. A. Heidenreich, M. P. Sajan, R. V. Farese, D. B. Stolz, P. Tso, S. H. Koo, M. Montminy, and T. G. Unterman.** 2006. FoxO1 regulates multiple metabolic pathways in the liver: effects on gluconeogenic, glycolytic, and lipogenic gene expression. J. Biol. Chem. **281:**10105–10117.